SUPPORTING INFORMATION

For

DYNAMIC STABILIZATION OF EXPRESSED PROTEINS IN ENGINEERED DIATOM BIOSILICA MATRICES

Yijia Xiong,[†] Nicole R. Ford,[‡] Karen A. Hecht,[‡] Guritno Roesijadi,[‡, §] and Thomas C. Squier[†]

[‡]Marine Biotechnology Group, Pacific Northwest National Laboratory, Sequim, WA 98382; [§]Department of Microbiology, Oregon State University, Corvallis, OR 97331, [†]Department of Basic Medical Sciences, Western University of Health Sciences, Lebanon, OR 97355

Table of Contents

ABBREVIATIONS

D_t, translational diffusion coefficient; D_r, rotational diffusion coefficient; EGFP, enhanced green fluorescent protein; PBS, phosphate buffered saline or 10 mM NaH_2PO_4 (pH 7.4), 137 mM NaCl, and 2.7 mM KCl; scFv, single chain fragment variable antibody; $sil3_{T8}$, lysine rich targeting sequence used to direct proteins to assemble within the biosilica frustule; TNB, trinitrobenzene; TNB-Alexa488 or TNB-Alexa555, fluorescent analogs of trinitrobenzene linked to either the Alexa488 or Alexa555 chromophore through cadaverine linkages; TNT, trinitrotoluene.

MATERIALS AND METHODS

*Alexa-TNB Synthesis***.** TNB-Alexa488 and TNB-Alexa555 were synthesized by conjugating TNB-sulfonic acid (Sigma-Aldrich) to either Alexa Fluor 488 cadaverine or Alexa Fluor 555 cadaverine (Life Technologies). Fluorescent ligands were purified using Supelclean LC-18 SPE columns[1] or by C-18 reversed phase high performance liquid chromatography (RP-HPLC) with an Agilent 1200 series HPLC, Synergi 4 µ Hydro-RP 80A, 250x10 mm column (Phenomenex), and a water/methanol gradient. Purity was verified as the elution of a single peak at the position of the respective TNB-Alex conjugate in analytical-scale C-18 RP-HPLC separations (4µ Hydro-RP 80A, 256 x 4.6 mm column [Phenomenex] and a water/methanol gradient) (Figure S1). The purified material exhibited the excitation and emission profiles characteristic of the respective Alexa fluorophore (http://dev.cose.isu.edu/bios/mrcf/aicf/resources/). TNB-Alexa488 was synthesized due to the published sensitivity of Alexa488 to the local environment,[1] and was capable of high-affinity binding to the scFv within transformed diatoms. TNB-Alexa555 was synthesized to reduce the contribution of light scattering.

Culture Conditions. Native and transformed cultures of *Thalassiosira pseudonana* (CCMP1335; Provasoli-Guillard National Center for Marine Algae and Microbiota) were maintained in artificial seawater (ESAW; https://ncma.bigelow.org/media/pdf/NCMA algal medium ESAW.pdf) supplemented with 100 µg/mL penicillin (VWR) and 100 µg/mL streptomycin (Sigma-Aldrich) on an orbital shaker under continuous illumination (~10-40 µmol/m^2/sec, 20-22 °C) or in a Caron plant incubator under continuous illumination (150 µmol/m^2/s; 20 °C) without agitation.

*Expression Clone Construction***.** Multisite Gateway Pro (ThermoFisher Scientific) cloning was used to construct a diatom-specific expression vector for the biosilica targeted $scFv_{TNT}$ fusion protein. In this $Sil3_{T8}$ construct, the N-terminal region of expressed proteins included a 17 amino acid ER targeting sequence (MKTSAIVLLAVLATTAA), a 23 amino acid linker sequence (GGAREACCKAEAACCTTLYNKVA), followed by a 39 amino acid $Sil3_{T8}$ coding sequence (KSKQGKTEMSVADAKASKESSMPSSKAAKIFKGKSGK) required for biosilica precipitation and targeting into the silica deposition vesicles (SDV). Insertion of a tagging sequence (AREACCKAEAACC) able to selectively bind cell-permeable AsCy3 biarsenical probes within the linker sequence permits site-specific protein labeling, as described previously.[2] The EGFP-containing construct is as previously described, with the same ER targeting sequence and $Sil3_{T8}$ peptide as the scFv-containing clone, but constructed with a linker sequence encoding GT.[2-4]

Transformation of Diatoms. Diatoms were transformed by microparticle bombardment with a PDS-1000/He particle delivery system (Bio-Rad) using established procedures with a 9 cm distance to the stopping screen and a 1550 psi rupture disk).[5] Tungsten microcarrier (M-17/~0.7 μm diameter; Bio-Rad) was coated with 10 μg supercoiled plasmid DNA using the $CaCl_2$-spermidine method.[2] Following transformation and selection, a single colony was isolated to enhance the homogeneity of the isolated diatom population.

Isolation of Diatom Biosilica. Diatom biosilica was isolated as previously described for detergent extraction at 50 °C,[6] substituting 1% Igepal CA-630 (Sigma) for 1% (w/v) SDS. For biosilica used in the fluorescence lifetime measurements, the isolation was conducted at 37°C with agitation for 60 min, followed by three additional extractions with agitation for 5 min at 37 °C, three water washes and one buffer wash [20 mM NaH_2PO_4 (pH 7.0) and 100 mM EDTA].[6]

Fluorescence Labeling of Frustules. Isolated frustules transformed with $Sil3_{T8}$-$scFv_{TNT}$ (1 x 10^8 frustules/mL) were incubated (1 hr) with TNB-Alexa488 or TNB-Alexa555 (50 μM) in phosphate buffered saline (PBS) containing 0.05% (v/v) Tween 20 and 0.05% (w/v) BSA at 4 °C, followed by 1 hour (25 °C) with gentle agitation. Frustules were washed three times with PBS + 0.05% (v/v) Tween 20 and re-suspended in PBS. The final concentration was about 5 x10^7 frustules/mL. When indicated, 8 M urea was included during labeling.

Absorption and Fluorescence Emission Spectra. All absorption spectra were taken on an Evolution 300 spectrophotometer (ThermoFisher Scientific; Waltham, MA). Fluorescence spectra were measured on a FluoroMax-2 fluorometer (Horiba Jobin Yvon; Albany, NY). For fluorescence measurements, the concentrations of fluorophores in solution were about 10 nM, while frustule concentration was 1 x 10^6 frustules/mL unless otherwise noted. In all cases, frustule concentrations were determined using microscopy to physically count frustules within aliquots added to a disposable hemocytometer C-Chip DHC-N01 (NanoEnTek,Pleasanton, CA). All measurements were made in PBS, unless otherwise mentioned. Integrated fluorescence emission spectra were used for all quantitative analysis.

Epifluorescence microscopy. Images of isolated frustules were captured with a Leica DM IRB inverted epifluorescence microscope equipped with a mercury metal halide light source with liquid light guide (Leica) and a CoolSNAP Myo camera (Photometrics). Filter cubes were used to collect fluorescence with the following settings for Ex/Em: (1) TNB-Alexa555, 532-552/572-642 nm and (2) EGFP, 460-500/512-542, nm. Images were captured with Metamorph software (v.7.7.11.0; Molecular Devices, Sunnyvale, CA).

Measurements of Binding Affinity. Fluorescence correlation spectroscopy (FCS) was used to measure the binding affinity between Alexa555-TNB and $scFv_{TNT}$, which involved assessing the rates of translational diffusion (D_t) for TNB-Alexa555 (0.5 nM) in the presence of variable amounts of $scFv_{TNT}$ (Figure S1). FCS measurements were collected in phosphate buffered saline (PBS)(10 mM phosphate (pH 7.4,) 2.7 mM KCl, 150 mM NaCl) with 0.05% Tween 20 (v/v) and 20% (v/v) glycerol, essentially as previously described.[7] Typically, accumulation times for each sample were 5 minutes.

Briefly, excitation involved a 532 nm diode pumped solid state laser (Laserglow Technology, Toronto, Canada) to excite TNB-Alexa555, where the laser power was 45 μW measured at the entry port of the microscope. Light was focused using a 60x objective lens (Fluo

Apo 60X VC, Nikon, Melville, NY) onto a spot 50 µm above the surface of a glass bottom fluorescence microplate (Greiner bio-one, Monroe, North Carolina). Fluorescence emission was collected using the same objective, separated by a z532/633rpc dichroic mirror and a HQ560/50 emission filter (ChromaTechnology, Bellows Falls, VT) and coupled into a 50 µm diameter optical fiber which also served as the pinhole. The fluorescence was sent to a pair of SPCM-AQR-14 avalanche photodiodes (Perkin-Elmer Optoelectronics, Vaudreuil, Canada) after a cube beam splitter (Thorlabs, Newton, NJ). The output of the avalanche photodiodes was fed into a Flex02-01D multi-tau correlator (Correlator.com, Bridgewater, NJ), and the fluorescence correlation curves were calculated in real time. The system was calibrated with a standard fluorophore R6G, whose diffusion coefficient was 4.1 x 10^{-6} cm^2/sec.[7]

Correlation curves were fit as previously described,[7,8] where the prolate shape of the foci permits the use of the following equation:

$$G(\tau) = 1 + \frac{1}{N}\left[(1-f)\cdot\frac{1}{1+\frac{\tau}{\tau_{Df}}} + f\cdot\frac{1}{1+\frac{\tau}{\tau_{Db}}}\right) \quad .$$

N is the total number of fluorescent molecules within the focus point, f is the fraction of TNB-Alexa555 bound to the scFv antibody, and τ_{Df} and τ_{Db} are the translational diffusion coefficients of TNB-Alexa555 in solution (free) and following binding to scFv. To construct a binding curve (Figure S1B), τ_{Df} and τ_{Db} were measured for TNB-Alexa555 in the absence and presence of excess scFv (i.e., 1 µM). The relationship between the translational diffusion time (τ_{Di}) and diffusion coefficient (D_i) is:

$$\tau_{Di} = \frac{\omega^2}{4Di} \quad ,$$

where ω is the radial radius of the laser focus point, τ_{Di} is the translational diffusion time of either the free (τ_{Df}) or bound (τ_{Db}) population, and D_t is the calculated translational diffusion coefficient. The dissociation coefficient K_d was fit to a Langmuir isotherm:

$$f = \frac{[scFv]}{K_d + [scFv]} \quad ,$$

where f is the fraction of TNB-Alexa555 bound to the scFv antibody, [scFv] is the unbound antibody concentration, and K_d is the apparent dissociation constant.

Frequency-Domain Fluorescence Measurements. The fluorescence lifetime and rotational dynamics of TNB-Alexa488 or TNB-Alexa555 were measured using an ISS K2 frequency domain fluorometer (Champaign, IL), as described previously.[9,10] Samples labeled with TNB-Alexa555 were excited using a 518 nm laser diode with fluorescence emission detected subsequent to a 540LP long-pass filter (Omega Optical, Brattleboro, VT). For EGFP and TNB-Alexa488 samples, excitation used a 488 nm laser diode with emitted light detected subsequent to an HQ535/50 band-pass filter (Chroma Technology Corporation, Bellow Falls, VT). For lifetime measurements, either rhodamine B (τ_{ref} = 1.7 ns) or fluorescein (τ_{ref} = 4.0 ns) were used as lifetime standards (http://www.iss.com/resources/reference/data_tables/

StandardsLEDsLaserDiodes.html). Scattering limited all lifetime measurements to frustule concentrations at or below 1×10^7 /mL. All measurements were taken at 25 °C.

Analysis of Fluorescence Lifetime Intensity Decays. The frequency domain fluorescence lifetime data were analyzed by fitting the time-dependent decay, I(t), of fluorescence to a sum of exponentials using nonlinear least-squares, as previously described.[11,12]

$$I(t) = \sum_{i=1}^{n} \alpha_i e^{-t/\tau_i}$$

where α_i values represent the pre-exponential factors, τ_i values represent the decay times, and *n* is the number of exponential components required to describe the decay. The intensity decay law is obtained from the frequency response of amplitude-modulated light and is characterized by the frequency-dependent values of the phase and the extent of demodulation. The values are compared with the calculated values from an assumed decay law until a minimum of the reduced squared deviation (χ_R^2) was obtained. After the measurement of the intensity decay, the mean lifetime was calculated:

$$\bar{\tau} = \sum_{i=1}^{n} \alpha_i \, \tau_i$$

Errors in the differential phase and modulated anisotropy were assumed to be 0.2° and 0.004, respectively. Weighted residuals were calculated as the difference between measured and fit data divided by the error of individual measurements (0.2° or 0.004 for phase shift and modulation data respectively).

Analysis of Fluorescence Anisotropy Decays. Time-resolved anisotropies were measured from the differential phase and modulated anisotropy, as previously described.[12] Anisotropy decays were fit to a sum of exponentials:

$$r(t) = r_o \, x \sum_{i=1}^{n} g_i \, e^{-t/\varphi_i} \ ,$$

where r_o is the limiting anisotropy in the absence of rotational diffusion, φ_i are the rotational correlation times, and g_i x r_o are the amplitudes of the total anisotropy loss associated with each correlation time. Parameter values were determined by minimizing the reduced chi-squared χ_R^2, and error surfaces were constructed for each rotational correlation time, which provides a conservative estimate of the recovered values.[13] Briefly, the values of χ_R^2 determined using a range of fixed rotational correlation time ϕ_i, (with all other parameters variable) were divided by the minimum value of $\chi_R^2(\text{min})$ obtained for the optimal fit. Typically, the normalized chi-squared (χ_N^2) is calculated as: $\chi_N^2 = \chi_R^2/\chi_R^2(\text{min})$, which facilitates comparison of different fitting parameters. Error ranges are calculated using the F-statistic for one standard deviation from the mean.

Theoretical Rotational Correlation Times. Assuming a solvent density of 1.0 g/mL and a viscosity of 0.01 Poise, the program Hydropro[14] was used to calculate the theoretical diffusion coefficient (D_r) of EGFP using the coordinates 4eul.pdb, which was found to be 1.096×10^{-7} sec^{-1}. The expected rotational correlation time (φ_r) is 15.2 nsec, assuming $\varphi_r = 1/6D_r$.

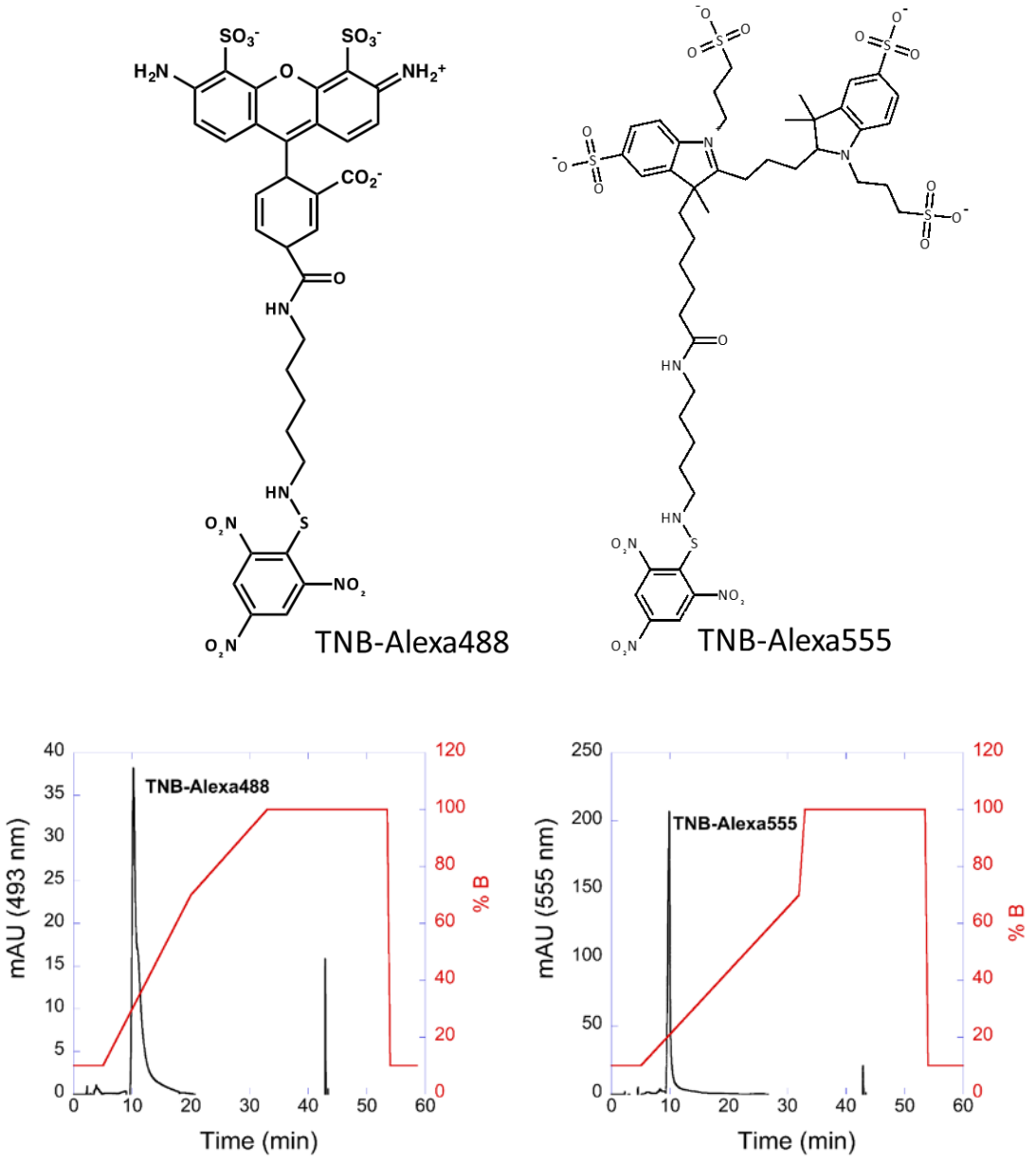

Figure S1: *HPLC Separation of Fluorescent Derivatives of TNT.* Structures (top panel) and chromatographic separation (bottom panels) of TNB-Alexa488 (left) and TNB-Alexa555 (right). TNB-sulfonic acid was conjugated to starting materials Alexa488 cadaverine (https://www.thermofisher.com/order/catalog/ product/A30676) or Alexa555 cadaverine (http://www.google.com/patents/US6977305; US patent #US6977305 B2). Chromatographic separation of TNB-Alexa488 (panel A) or TNB-Alexa555 (panel B) by reversed-phase HPLC using a C-18 RP column and a water (solvent A)/methanol (solvent B) gradient. Elution profiles were monitored at the absorption maxima for the respective TNB-Alexa conjugates.

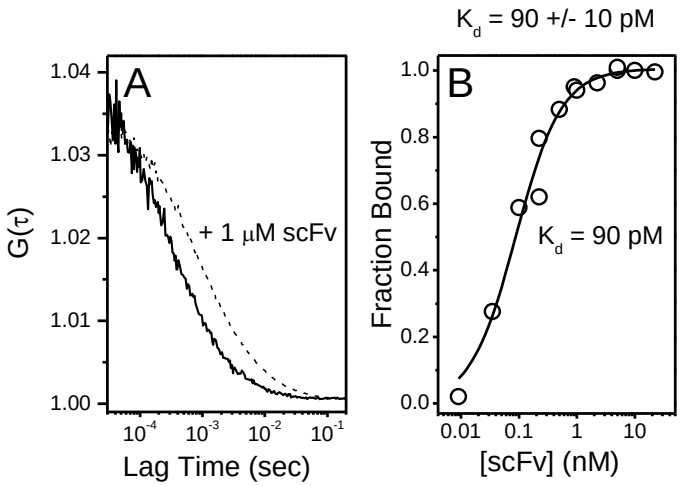

Figure S2: *High-Affinity Binding of TNB-Alexa555 to scFv in Solution*. (*Panel A*) Representative fluorescence correlation curves for TNB-Alexa555 (0.5 nM TNB) in the absence (thick solid line) and presence (thin dashed line) of scFv (1 μM). Calculated translational diffusion coefficients (D_t) are 2.2 x10^{-6} cm^2/s (TNB-Alexa555) and 0.62 x10^{-6} cm^2/s (TNB-Alexa555 + scFv), representing an increase in mass of 30 kDa upon scFv binding to TNB-Alexa555. (*Panel B*) Nonlinear least-squares fit to Langmuir binding isotherm (solid line; K_d = 90 ± 10 pM) using FCS binding curves to calculate fraction of TNB-Alexa555 bound to scFv (open circles), as described in Methods. Measurements were made in PBS with 20% (v/v) glycerol and 0.05% (v/v) Tween 20 at 25 °C. λ_{ex} = 532 nm; emitted light was collected subsequent to a HQ560/50 bandpass filter (Chroma Technology Corporation, Bellow Falls, Vt.).

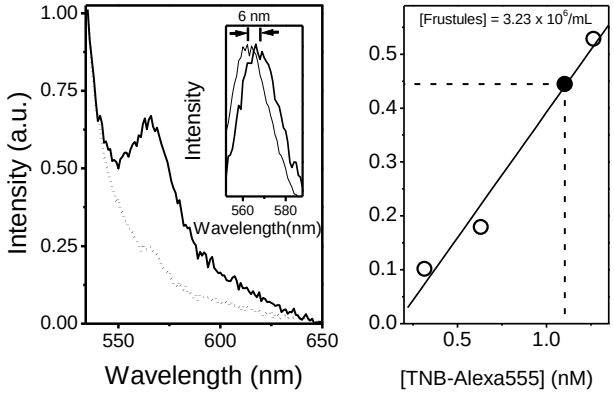

Figure S3: *Determination of Maximal Concentration of scFv Tethered in Frustule Biosilica*. (*Left Panel*) Fluorescence emission spectra (λ_{ex} = 518 nm) for transformed frustules expressing scFv following incubation with TNB-Alexa555 (50 μM) and removal of unbound dye (solid line) relative to frustules in the absence of added TNB-Alexa555 (dotted line). Inset shows 6 nm red shift in fluorescence of TNB-Alexa555 upon binding scFv tethered in frustule biosilica (solid thick line) relative to TNB-Alexa555 in solution. (*Right Panel*) Standard curve showing relationship between fluorescence intensity and TNB-Alexa555 concentration, permitting a determination of the concentration of scFv in transformed diatom frustules (1.1 nM), which corresponds to 205,000 scFv antibodies in each frustule (3.23 x 10^6 frustules per mL). All measurements were made in PBS at 25 °C.

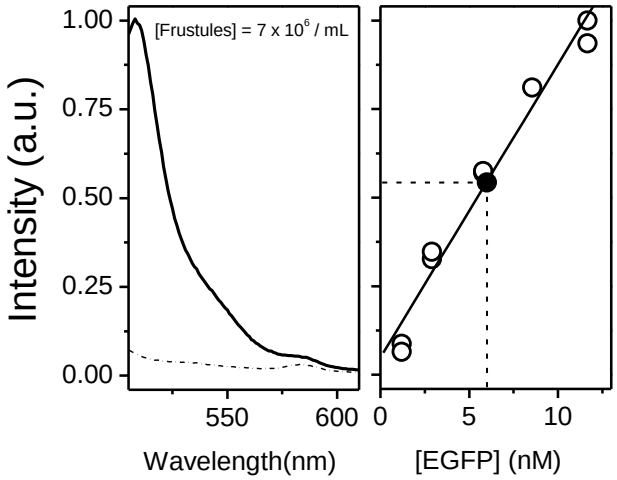

Figure S4: *Determination of Concentration of EGFP Tethered in Frustule Biosilica*. (*Left Panel*) Fluorescence emission spectra (λ_{ex} = 488 nm) for transformed frustules expressing EGFP (solid line) relative to wild-type frustules (dot-dashed line). (*Right Panel*) Standard curve showing relationship between fluorescence intensity and EGFP concentration, permitting a determination of the concentration of EGFP in transformed diatom frustules (6.0 nM), which corresponds to 530,000 EGFP in each frustule (7 x 10^6 frustules per mL). All measurements were made in PBS at 25 °C.

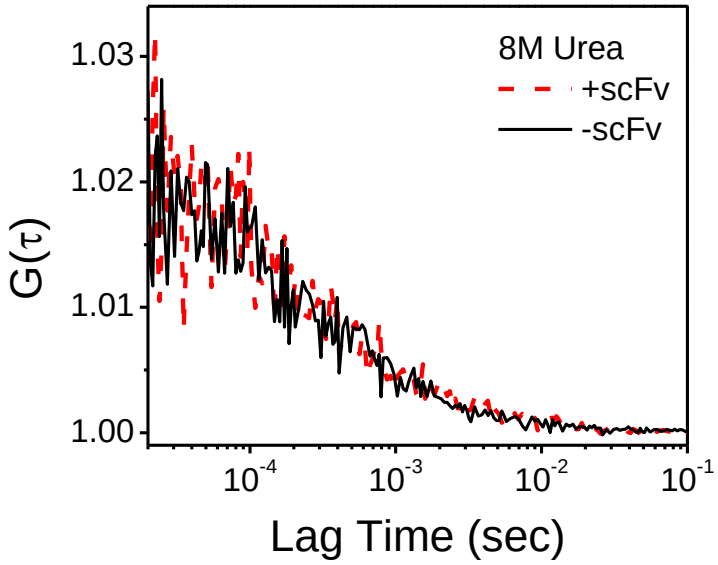

Figure S5: *Loss of TNB-Alexa555 Binding to scFv in solution upon addition of 8M Urea*. Representative fluorescence correlation curves for TNB-Alexa555 in the absence (solid black line; τ_D = 250 ± 20 μs) and presence (dashed red line; τ_D = 260 ± 20 μs) of scFv (1 μM) in 50 mM HEPES (pH = 7.5), 0.15 M NaCl, 10 mM $CaCl_2$, 0.02% (v/v) Tween 20, and 8 M urea at 25 °C. Fluorescence emission was collected subsequent to a HQ560/50 bandpass filter (Chroma Technology Corporation; Bellow Falls, Vt.). λ_{ex} = 532 nm

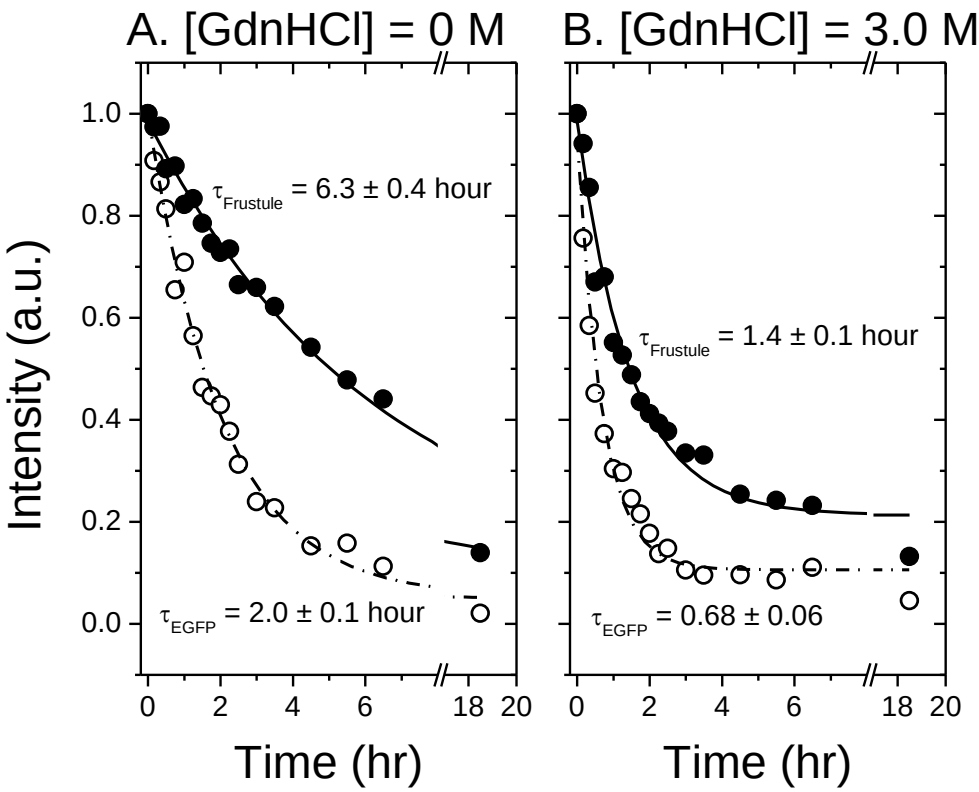

Figure S6: *Increased Stability of EGFP Tethered in Frustule Biosilica*. Time-dependent changes in fluorescence intensity (integrated intensity between 510 and 535 nm) (λ_{ex} = 488 nm) for EGFP in solution (open circles; 3.5 nM) and tethered in frustule biosilica (closed circles; 900,000 frustules/mL) in PBS in the absence (panel A) and presence (panel B) of 3 M guanidine hydrocholide. Temperature = 25 °C.

REFERENCES:

(1) Lindhoud, S., Westphal, A. H., Visser, A. J., Borst, J. W., and van Mierlo, C. P. (2012) Fluorescence of Alexa fluor dye tracks protein folding. *PloS One 7*, e46838.

(2) Ford, N. R., Hecht, K. A., Hu, D., Orr, G., Xiong, Y., Squier, T. C., Rorrer, G., and Roesijadi, G. (2016) Antigen binding and site-directed labeling of biosilica-immobilized fusion proteins expressed in diatoms. *ACS Synthetic Biology 5*, 193-199.

(3) Liu, J. L., Zabetakis, D., Acevedo-Velez, G., Goldman, E. R., and Anderson, G. P. (2013) Comparison of an antibody and its recombinant derivative for the detection of the small molecule explosive 2,4,6-trinitrotoluene. *Analytica Chimica Acta 759*, 100-104.

(4) Poulsen, N., Scheffel, A., Sheppard, V. C., Chesley, P. M., and Kröger, N. (2013) Pentalysine clusters mediate silica targeting of silaffins in Thalassiosira pseudonana. *J. Biol. Chem.* 288, 20100-20109.

(5) Poulsen, N., Chesley, P. M., and Kröger, N. (2006) Molecular genetic manipulation of the diatom *Thalassiosira pseudonana* (Bacillariophyceae). *J. Phycology 42*, 1059-1065.

(6) Poulsen, N., Berne, C., Spain, J., and Kröger, N. (2007) Silica immobilization of an enzyme through genetic engineering of the diatom *Thalassiosira pseudonana*. *Angewandte Chemie-International Edition 46*, 1843-1846.

(7) Xiong, Y., Chen, B., Smallwood, H. S., Urbauer, R. J., Markille, L. M., Galeva, N., Williams, T. D., and Squier, T. C. (2006) High-affinity and cooperative binding of oxidized calmodulin by methionine sulfoxide reductase. *Biochemistry 45*, 14642-14654.

(8) Muller, C. B., Loman, A., Pacheco, V., Koberling, F., Willbold, D., Richtering, W., and Enderlein, J. (2008) Precise measurement of diffusion by multi-color dual-focus fluorescence correlation spectroscopy. *Europhysics Letters 83*, 46001.

(9) Gratton, E., and Limkeman, M. (1983) A continuously variable frequency cross-correlation phase fluorometer with picosecond resolution. *Biophysical journal 44*, 315-324.

(10) Lakowicz, J. R., and Maliwal, B. P. (1985) Construction and performance of a variable-frequency phase-modulation fluorometer. *Biophys. Chem. 21*, 61-78.

(11) Bevington, P. R. (1969) *Data Reduction and Error Analysis for the Physical Sciences*, McGraw-Hill, New York.

(12) Hunter, G. W., and Squier, T. C. (1998) Phospholipid acyl chain rotational dynamics are independent of headgroup structure in unilamellar vesicles containing binary mixtures of dioleoyl-phosphatidylcholine and dioleoyl-phosphatidylethanolamine. *Biochim. et Biophys. Acta 1415*, 63-76.

(13) Beechem, J. M., and Haas, E. (1989) Simultaneous determination of intramolecular distance distributions and conformational dynamics by global analysis of energy transfer measurements. *Biophys J. 55*, 1225-1236.

(14) Ortega, A., Amoros, D., and Garcia de la Torre, J. (2011) Prediction of hydrodynamic and other solution properties of rigid proteins from atomic- and residue-level models. *Biophys. J. 101*, 892-898.